StrathE2E2 version 3.3.0: Ecology model description.

Michael R. Heath & Douglas C. Speirs

Department of Mathematics and Statistics, University of Strathclyde, Glasgow, UK.
E-mail: m.heath@strath.ac.uk

Date: October 2020

Introduction

The StrathE2E2 ecology model builds on an earlier fully documented prototype (StrathE2E1; Heath, 2012), by adding additional state variables and horizontal spatial differentiation to better represent natural ecology and anthropogenic disturbances. This document describes the features which extend StrathE2E2 from the earlier prototype, in particular:

- Horizontal spatial structure in the water column and seabed, including the representation of multiple discrete seabed sediment types and their natural and anthropogenic disturbance,
- Representation of fast and slow degrading organic matter in sediments,
- Dynamics of macrophytes (kelp),
- Dynamics of planktonic larval stages of benthic fauna,
- Dynamics of migratory fish which undergo seasonal immigration and emigration from the model domain,
- Differentiation of the previously combined bird & mammal top predator guild in the model into birds, seals (pinnipeds) and cetaceans,
- Production of detritus and corpses by mortality of phytoplankton, zooplankton, planktonic larvae, and benthos,
- Appropriate representation of feeding and temperature dependence for top-predators,
- Passive transport of detritus, nutrients and plankton between internal spatial compartments of the model,
- Active migrations of fish and top-predators between internal spatial compartments of the model,
- Parameterisation of the proportion of resource guild biomass which is accessible to fishing gears.

Brief summary of the prototype model

Full details of the StrathE2E1 prototype model are provided elsewhere (Heath 2012), and only the basic details are provide here.

In terms of the physical structure, StrathE2E1 represented a 1-dimensional (vertical) water/sediment column with two water layers and a single homogeneous sediment layer i.e. no horizontal compartmentalisation or sediment heterogeneity. Regarding state variables, the key differences between StrathE2E1 and StrathE2E2 are shown below and in **Tables 1 and 2**.

Key developments of the ecological terms in the model between the prototype (Heath 2012) and the new StrathE2E2:

- Division of sediment detritus into labile and refractory fractions, and improved representation of seabed disturbance

- Representation of macrophytes (absent in the prototype)
- Representation of larval stages of benthos guilds (absent in the prototype)
- Representation of migratory fish (absent in the prototype)
- Disaggregation of the combined bird & mammal guild in the prototype into birds, pinnipeds and cetaceans

Key developments in spatial granularity of the model between the prototype (Heath 2012) and the new StrathE2E2
- Division of the model domain into offshore and inshore zones
- Division of seabed sediments into multiple types

Key developments in the representation of fishing in the model between the prototype (Heath 2012) and the new StrathE2E2
- Development of a separate fishing fleet model linked to the ecology model
- Improved representation of discarding, offal production and seabed disturbance by fishing operations

Table 1. Ecology model state variables and spatial hierarchy in the StrathE2E1 prototype model (Heath 2012)

Differentiated by vertical layer (sediment or water column)	Represented as depth integrated mass but with dynamic vertical distribution	Represented as depth integrated mass
Sediment bacteria and labile detritus	Omnivorous zooplankton	Fishery discards
Suspended bacteria and detritus	Carnivorous zooplankton	Corpses
Pore-water nitrate		Larvae of planktivorous fish
Pore-water ammonia		Larvae of demersal fish
Water column nitrate		Suspension/deposit feeding benthos
Water column ammonia		Carnivore/scavenge feeding benthos
Phytoplankton		Planktivorous fish
		Demersal fish
		Birds & mammals

Description of the StrathE2E2 ecology model

Table 2. Ecology model state variables and spatial hierarchy in StrathE2E2

Differentiated by horizontal zone and sediment habitat	Differentiated by horizontal zone and water column layer	Differentiated by horizontal zone with modelled vertical distribution	Differentiated by horizontal zone only
Sediment bacteria and labile detritus	Nitrate	Omnivorous zooplankton	Suspension/deposit feeding benthos
Refractory sediment detritus	Ammonia	Carnivorous zooplankton	Carnivore/scavenge feeding benthos
Pore-water nitrate	Suspended bacteria and detritus	Larvae of suspension/deposit feeding benthos	Planktivorous fish
Pore-water ammonia	Phytoplankton	Larvae of carnivore/scavenge feeding benthos	Demersal fish (divided into fishery quota-limited and non-quota components)
Fishery discards		Larvae of planktivorous fish	Migratory fish
Corpses		Larvae of demersal fish	Pinnipeds
Macrophytes (confined to inshore rock habitat)			Seabirds
			Cetaceans

Key equations in StrathE2E2

The general equation for the rate of change of a food web component (X) in StrathE2E2 given a set of k prey types (N_k) and a set of j predator types (Y_j), is essentially the same as in the prototype, with the exception of the uptake function for the birds and mammals:

$$\frac{dX}{dt} = A \sum_k U_{X(N_k)} - \sum_j U_{Y_j(X)} - \varepsilon(t)X - \delta X^2 + F_X - H(t)X - D(t)X + R_X \qquad \text{eqn 1}$$

$U_{v_1(v_2)}$ Flux of ingestate to a predator (v_1) from prey (v_2). ($v_1, v_2 = X, N$ or $v_1, v_2 = Y, X$)

A Assimilation efficiency. Ingestate not assimilated ($(1-A) \sum_k U_{X(N_k)}$) is divided equally between a flux to dissolved ammonia, and a flux to detritus.

$\varepsilon(t)$ Temperature, and hence time-dependent basal metabolic rate coefficient (generates a flux from body mass to ammonia)

Δ Density dependent mortality coefficient (generates a flux from body mass to a detritus category)

F_X Vertical advection and diffusion fluxes affecting the food web component

$H(t)$ Harvest ratio (time-dependent rate of biomass capture by fisheries)

$D(t)$ Time-dependent developmental export rate for the food web component X. For X = adult stages, $D(t)X$ represents the flux of spawning products to the egg, larval and juvenile (ELJ) stage. For X = ELJ stages, $D(t)X$ represents the settlement flux to adults. For food web components lacking demographic structure, $D(t) = 0$

R_X Recruitment flux to the food web component X. For X = adult stages, R_X is equal to the settlement flux from the ELJ stage. For X = ELJ stages R_X is equal to the

flux of spawning products from the adults. For food web components lacking demographic structure, $Rx = 0$

General equation for the flux of ingestate to a predator (v_1) from prey (v_2) is:

$$U_{v_1(v_2)} = \frac{v_1.v_2.\rho_{v_1(v_2)}.Umax_{v_1}}{v_2 + h_{v_1}}$$

eqn 2

$\rho_{v_1(v_2)}$ Preference of the predator v_1 for the prey class v_2. For a given predator class, the sum of the preference coefficients over all prey classes = 1.

$Umax_{v_1}$ Temperature, and hence time-dependent maximum uptake rate of the predator v_1

h_{v_1} Half-saturation constant for uptake of prey by the predator v_1 (temperature independent)

For phytoplankton (v_1 = phytoplankton $(X = P)$), the assimilation efficiency $A = 1$, temperature dependent basal metabolic rate coefficient $\varepsilon = 0$, and there is no demographic structure so $D(t) = 0$ (and hence $R_X = 0$). The uptake of prey (v_2 = dissolved nutrient N_k) has a light-dependent term:

$$U_{P(N_k)} = Min\left\{1, \frac{L(t)}{L_{max}}\right\} \frac{P.N_k.\rho_{P(N_k)}.Umax_P}{N_k + h_P}$$

eqn 3

$L(t)$ Time-dependent light intensity
L_{max} Saturation light intensity for nutrient uptake

In the prototype model, food uptake of the combined bird & mammal guild followed the Michelis Menten form outlined above for all other living guilds. In StrathE2E2, uptake of prey by the top-predators (birds, pinnipeds and cetaceans), follows the predator-density dependent Beddington-DeAngelis functional form (Beddington, 1975; DeAngelis *et al.,* 1975) with an additional parameter γ:

$$U_{v_1(v_2)} = \frac{v_1.v_2.\rho_{v_1(v_2)}.Umax_{v_1}}{v_2 + \gamma v_1 + h_{v_1}}$$

eqn 4

Justification of the Beddington-DeAngelis form is presented later in this document.

Representing horizontal structure, seabed habitats and sediment processes

We define two depth-zones of seabed in StrathE2E2 – an inshore/shallow/well-mixed zone and an offshore/deep/seasonally-stratified zone. We use the terms 'inshore' and 'offshore' to refer to these zones though it should be noted that, in reality, shallow well-mixed areas of a model region can be located over isolated offshore banks as well as adjacent to the coast. However, we assume that for the purposes of the model the inshore zone constitutes a contiguous, horizontally homogeneous body of water.

The inshore zone comprises a single water column layer connected vertically to a seabed sediment later. The latter is divided horizontally into to four habitats defined by sediment properties. The offshore zone has two vertically connected water column layers (upper and lower), with the lower being connected to seabed sediment habitats as in the shallow zone. The offshore zone upper layer and the shallow zone are horizontally connected to represent advection and mixing. This arrangement is in contrast to the prototype model which comprised two vertical water column layers and a single homogeneous sediment layer.

Resolving different types of sediments

The extents of seabed habitats in each zone are defined by their area-proportion of the seabed. One habitat in each zone is reserved for exposed rock, and the other three are configurable for any combination of sediment types defined by layer thickness, median grain size, porosity, hydraulic conductivity and natural disturbance rate. Data on sediment porosity and hydraulic conductivity are scarce, so the model code includes an option to impute these from median grain size values using default or user-supplied parameters.

Porosity is the proportion by volume of the sediment which is fluid-filled void space, and is typically highest in fine-grained sediments. In the model, porosity is a scaling factor linking pore-space volume to whole-sediment layer volume, so that nutrient concentrations can be expressed in terms of pore-water volume.

Hydraulic conductivity (m.s^{-1}) represents the ease with which fluids flow through the particle grain matrix of the sediment and is equivalent to the diffusion velocity. The related and more often quoted term 'permeability' (m^{-2}) is a measure of the connectedness of the fluid filled void spaces between the particle grains. Permeability is a function only of the sediment matrix, whilst conductivity is a function of both the sediment and the permeating fluid, in particular the fluid viscosity and density.

Hydraulic conductivity is related to permeability by:

$$H = Permeability \cdot fluid\ density \cdot \frac{g}{dynamic\ viscosity} \qquad \text{eqn 5}$$

where: seawater density = 1027 kg.m^{-3} at salinity 35 and temperature 10°C; seawater dynamic viscosity = 1.48 x 10^{-3} kg.m^{-1}.s^{-1} at salinity 35 and temperature 10°C; g = acceleration due to gravity = 9.8 m.s^{-1}

Hence, $H = Permeability \cdot 6.8004\ x\ 10^6$ (m.s^{-1} at salinity 35 and temperature 10°C)   eqn 6

Derivations of relationships between porosity, permeability and median grain size are provided in a separate document on the implementation of StrathE2E2 for the North Sea. Parameters of these relationships are probably sufficiently generic to be applicable in other shelf sea regions.

Representing sediment diagenesis and nutrient fluxes, and the effects of natural and anthropogenic disturbance

Detailed modelling of sediment diagenesis and nutrient fluxes requires dynamic resolution of the vertical gradients of dissolved and particulate nutrient and organic matter concentrations, oxygen and redox potential. This is usually modelled by multiple discrete vertical layers, or in continuous space by systems of partial differential equations (Arndt *et al.,* 2013). In line with the highly aggregated structure and taxonomy of the rest of StrathE2E2, we adopt a simpler but obviously cruder approach involving a single vertically homogeneous sediment layer in each habitat, and represent only the dynamics of organic and inorganic nitrogen.

As a starting point, the flux (Moles.m^{-2} sediment surface.d^{-1}) of a dissolved nutrient into or out of a sediment patch due to diffusion and hydraulic flow through the sediment-water interface, is given by the product of whole-sediment hydraulic conductivity, and the difference in concentration between whole-sediment interstitial pore-waters and the overlying water column:

$$H \cdot \left(\frac{n}{\gamma \cdot \varphi \cdot \delta} - \frac{N}{\Delta} \right)$$ <div style="text-align:right">eqn 7</div>

where, H is the hydraulic conductivity (m.d^{-1}), γ is the proportion of total seabed area occupied by the sediment patch, δ and Δ (m) are the thicknesses of the sediment layer and the overlying water column layer respectively, n and N are the masses (Moles) of nutrient in the sediment pore waters and the water column respectively, and φ is the sediment porosity. Positive values of the flux imply net flow from the sediment to the water column, and vice-versa.

Now, we introduce a process which erodes a proportion α of the sediment patch volume per day. This might entail the wholesale re-suspension of a skin of a given thickness, or bedload transport such as in the formation ripples and waves, or ploughing of a fraction of the patch surface area to a given depth. In each case, it is assumed that pore water of volume ($\alpha.\gamma.\varphi.\delta$) in the eroded sediment is replaced with an equivalent volume from the overlying water column. Assuming that the water column and pore waters are well mixed, we can represent this process as an enhancement of the hydraulic conductivity. The enhanced flux between the sediment patch and the water column is given by:

$$H \cdot \left(\frac{n}{\gamma \cdot \varphi \cdot \delta} - \frac{N}{\Delta} \right) + (\alpha \cdot n) - \frac{\alpha \cdot \gamma \cdot \varphi \cdot \delta \cdot N}{\Delta}$$ <div style="text-align:right">eqn 8</div>

which simplifies to:

$$\left(H + (\alpha \cdot \gamma \cdot \varphi \cdot \delta) \right) \cdot \left(\frac{n}{\gamma \cdot \varphi \cdot \delta} - \frac{N}{\Delta} \right)$$ <div style="text-align:right">eqn 9</div>

With respect to organic detritus re-suspended from the seabed along with the mineral material, the flux to the water column is simply $\alpha.d$, where d is the mass of detritus in the sediment, since the re-settlement flux is disconnected from the erosion process and already represented in the model.

The proportion α of a sediment patch volume which is disturbed per unit time is assumed to be made up of three components: physical erosion by bed shear stress due to currents and wave orbital velocities ($\alpha_{erosion}$), bioturbation by benthic fauna ($\alpha_{bioturb}$), and seabed abrasion or ploughing by trawling gears ($\alpha_{trawling}$). In each case, we need to estimate a partial value for the proportion of sediment volume disturbed due to the action of the process concerned. The total proportion of sediment volume disturbed is then the sum of the three components.

Natural disturbance

The area-proportion of each sediment habitat which is eroded by natural bed shear stress due to currents and waves needs to be derived independently and supplied to the model as driving data (annual cycle of monthly average values for each habitat – see separate document on the North Sea demonstration model for an example). We assume that erosion affects a surface skin of fixed thickness, so that volume-proportion of sediment eroded ($\alpha_{erosion}$) is simply the product of area-proportion and skin thickness.

Bioturbation

Burrowing and filter feeding benthic in-fauna create ventilation shafts into the interior of the sediment layer on the seabed and over-turn of the sediment structure. In effect, this process leads to an increased whole-sediment permeability and causes changes in nutrient fluxes

(Olsgard *et al.*, 2008), but we assume it does not lead to re-suspension of organic detritus. In the model we represent this phenomenon by linking the proportion of sediment disturbed per day to the daily proportion of sediment detritus consumed per day by the filter and deposit feeding benthos guild, with a scaling coefficient:

$$\alpha_{bioturb} = \beta_{bioturb} \cdot \frac{Uptake(d_{bs})}{d}$$ eqn 10

where $\beta_{bioturb}$ is a proportionality scaling factor, d denotes the mass of organic detritus in the sediment (dynamic and static detritus combined), $Uptake(d_{bs})$ denotes the daily uptake of organic detritus (dynamic and static detritus combined) by suspension and deposit feeding benthos.

The proportion of sediment disturbed by bioturbation, $\alpha_{bioturb}$, is applied only to the flux of dissolved nutrients between pore water and the water column, not to the resuspension flux of organic detritus.

Trawling disturbance

In the model we consider that ploughing or abrasion of the seabed by trawling gear mines out a proportion of the sediment volume in a habitat patch, and the porewater and organic matter contained therein is exchanged with the overlying water column. The proportion of seabed area abraded per day (p_T) in each sediment habitat is an output from the fishing fleet model. To this, we apply an assumed penetration depth of the gears into the sediment (x_T) to derive the proportion of sediment volume disturbed:

$$\alpha_{trawling} = p_T \cdot x_T$$ eqn 11

Modelling of organic detritus in marine sediments

Representing the return of nutrient to the water column as a result of organic matter mineralization in sediments is fundamental for any model which aims to represent a closed food web in shelf seas. However, this is a notorious problem in marine models. In common with many other models, the prototype for StrathE2E2 (Heath, 2012) assumed a closed boundary at the base of the sediment layer, and included a single dynamic category of sediment detritus with a temperature dependent first-order rate process determining the conversion of its organic nitrogen content to ammonia (see review by Arndt *et al.,* 2013). The parameter optimisation scheme implied a rate coefficient of 0.008 d^{-1} at 10°C which compared favourably with evidence from experiments conducted on recently deposited organic matter. However, this representation and parameterisation had several consequences that did not accord well with reality. In particular, the simulated weight-specific organic nitrogen content of sediment showed strong seasonal variation, and the predicted annual mean was less than 10^{-5} g.g^{-1}. In contrast, empirical data from the upper 5-10cm of temperate shelf sediments show little seasonal variation in total organic nitrogen content and annual average values which are at least an order of magnitude higher than in the model (around 10^{-4} g.g^{-1}). Nevertheless, observed concentrations of phyto-detritus pigments in sediments do show seasonal variation similar to that displayed by the prototype model (*e.g.* Serpetti *et al.,* 2012; Serpetti *et al.*, 2016). The implication is that the majority of organic matter in the sediments is not recently formed detritus, but more ancient material with a significantly slower decay rate (Arndt *et al.,*2013; Canfield, 1994). If slowly degrading material plays any role in the food web, then the prototype model has over-tight coupling between deposition fluxes, dissolved nutrient fluxes, and availability of food for detritivores.

Chemical analysis shows that organic matter in marine surficial sediments is composed of a range of compounds differing widely in their resistance to lysis by bacteria (Arndt *et al.*, 2013). Freshly deposited autochthonous material from the water column, especially phyto-detritus, contains highly labile fractions, but the residues which remain as the material ages are increasingly refractory, with degradation rates several orders of magnitude slower than the labile fraction. In undisturbed sediments the proportion of slowly degrading 'refractory' material increases with depth reflecting burial over time. A variety of processes are known to affect these progressive transformations including oxygen saturation, physical protection afforded by adsorption onto inorganic particles, transport of material within the sediment by bioturbation and physical disturbance, modification by detritivorous macrobenthos, and priming of refractory degradation rates by deposition fluxes of labile material. However, mechanistic understanding is poor and there is no consensus on detailed dynamic modelling of the organic chemistry of sediments, in particular on any mechanisms internal to the sediment which might regulate the mineralisation of refractory material, and hence the long-term burial rate.

Representing processes with rate constants smaller than around 10^{-4} d^{-1}, as seems likely for refractory organic matter, is problematic for a model such as StrathE2E2 which has an intrinsic daily resolution and is designed to respond to annual cycles of external driving data. Hence we simplified the problem of mineralisation by dividing the process into two parts (e.g. Billen, 1982); a fully dynamic part representing the rapid degradation of fresh organic matter, and a semi-dynamic part to represent fluxes related to the slow degradation of the mass of more refractory material accumulated over long periods of time. In effect, the semi-dynamic part constituted an open boundary condition within the sediment and allowed for an implicit burial flux of organic nitrogen.

For each sediment type in the model, a fixed mass of slowly decaying (refractory) organic nitrogen is defined, based on empirical data. This static organic nitrogen pool is involved in three flux processes within the model, the combination of which generates a net sink or source of nitrogen within the sediment.

- A flux of nitrogen from the static pool to sediment porewater ammonia is derived by applying a first-order rate parameter to the static pool, but with no depletion of the resource. The rate parameter is a constant proportion (order of magnitude 1%) of the temperature-dependent mineralisation rate applied to dynamic detritus,

- The static pool is also regarded as being available to deposit-feeding benthos in the model, but only a fraction is able to be digested. The digestible fraction is assimilated into biomass with the same efficiency as other ingested food, and contributes to the defecation and excretion flux of labile detritus and ammonia. The indigestible fraction is defecated directly back to environment unaltered, so is effectively a ballast fraction of the ingested material.

- Finally, refractory organic matter is produced within the food web as a stoichiometric by-product of the degradation of fast decaying (labile) sediment detritus, corpses and macrophyte (kelp) debris (see later section). Temperature-dependent decay of labile sediment detritus produces ammonia and refractory material in fixed proportions. Similarly, the temperature-dependent decay of corpses and macrophyte (kelp) debris produces suspended detritus and refractory detritus, again in fixed proportions. This representation of the complex processes of degradation encapsulates the progressive exposure of molecules which are resistant to lysis, and the production of refractory residues from dead bacteria.

Since the mass of refractory material is defined as constant, mineralisation and net ingestion by detritivores constitute boundary influxes to the model, whilst production within the food web constitutes a boundary sink. The net boundary flux will depend on the relative magnitudes of these three terms.

Equations for the sediment sub-model.

State variables in or associated with the sediment (units: mMN.m^{-2}):

D_{sed_f} fast-degrading labile sediment detritus
D_{sed_s} slowly-degrading refractory detritus
AM_{pw} ammonia in pore-waters
B_{fd} filter and deposit feeding benthos
C corpses of organisms
K macrophyte (kelp) debris

Intermediate flux terms (mMN.m^{-2}.d^{-1})

S_D Settlement flux of suspended detritus from the water column
R_D Resuspension flux of fast-degrading detritus from the sediment
F_A Diffusion flux of ammonia between sediment and water column
E_{Bfd} Defecation flux from filter/deposit feeding benthos
E_{Bcs} Defecation flux from carnivore/scavenge feeding benthos
$U_{Bfd,(Dsed\_f)}$ Consumption of labile detritus by filter/deposit feeding benthos
$U_{Bfd,(Dsed\_s)}$ Consumption of refractory detritus by filter/deposit feeding benthos
$U_{Bfd,(DWC)}$ Consumption of suspended detritus by filter/deposit feeding benthos
$U_{Bfd,(P)}$ Consumption of phytoplankton by filter/deposit feeding benthos

Parameters

$z(T)$ Temperature dependent disintegration rate of corpses (d^{-1})
$\delta(T)$ Temperature dependent disintegration rate of kelp debris (d^{-1})
$m(T)$ Temperature dependent mineralisation rate of labile sediment detritus (d^{-1})
$n(T)$ Temperature dependent nitrification rate of pore-water ammonia (d^{-1})
A Assimilation efficiency of filter/deposit feeding benthos
α Proportion of corpse, kelp debris, and labile detritus decay products classed as refractory
β Ratio of refractory to labile detritus mineralisation rates at the same temperature
φ Proportion of refractory detritus ingestate which is digestible by filter/deposit feeding benthos

Balance equations

$$\frac{dD_{sed\_f}}{dt} = S_D - R_D + E_{Bfd} + E_{Bcs} - U_{Bfd,(Dsed_f)} - m(T).D_{sed\_f} \qquad \text{eqn 12}$$

$$\frac{dAM_{pw}}{dt} = (1 - \alpha).m(T).D_{sed\_f} + \beta.m(T).D_{sed\_s} + F_A - n(T).AM_{pw} \qquad \text{eqn 13}$$

$$\frac{dD_{sed\_s}}{dt} = 0 \qquad \text{eqn 14}$$

Defecation flux of filter/deposit feeding benthos

$$E_{Bfd} = \frac{(1-A)}{2}\left(U_{Bfd,(P)} + U_{Bfd,(D_{WC})} + \varphi.U_{Bfd,(Dsed\_s)} + U_{Bfd,Dsed\_f)}\right) \qquad \text{eqn 15}$$

Hence the open boundary flux within the sediment is given by:

$$\beta.m(T).D_{sed\_s} + \delta.U_{Bfd,(Dsed_s)} - \alpha.m(T).D_{sed_f} - \alpha.z(T).C - - \alpha.\delta(T).K \qquad \text{eqn 16}$$

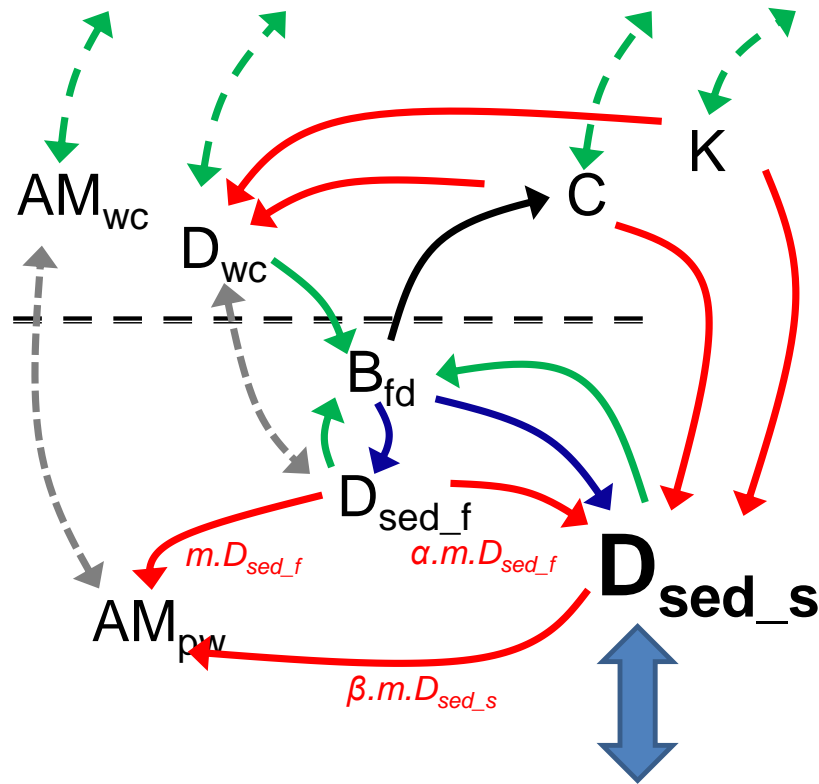Positive values of this flux indicate net inflow to the model, and vice versa.

FIGURE 1 Schematic of detritus transformation processes in the model sediment. For simplicity, the connections to the rest of the food web, in particular to carnivore/scavenge feeding benthos and to phytoplankton, are not shown in detail (double-ended green dashed arrows). Red arrows: microbial processes; green arrows: feeding fluxes; blue arrows: defecation fluxes; black arrows: mortality fluxes; grey dashed arrows: physical fluxes. The double-ended block arrow indicates the open boundary flux of nitrogen. State variable pools shown are fast degrading labile sediment detritus (D_{sed_f}); suspended detritus in the water column (D_{WC}); ammonia in pore-waters (AM_{pw}) and in the water column (AM_{WC}); corpses of organisms (C); macrophyte (kelp) debris (K); filter and deposit feeding benthos (B_{fd}), and the pool of slowly degrading refractory detritus (D_{sed_s}).

Scaling of sediment microbiology rates to sediment properties

Implementation of multiple seabed habitat types implied an equivalent number of values for each geochemical rate process parameter to distinguish between different sediment types. To reduce this parameter requirement, a single value for each process parameter is defined

at a reference hydraulic conductivity (*i.e.* a reference sediment grain size), and linked to the hydraulic conductivity specified for each sediment habitat by sensitivity parameters. The latter are set so that denitrification rates decline with increasing hydraulic conductivity (*i.e.* higher rates in muds than in sands and gravels), and vice-versa for mineralisation and nitrification. All rate parameters are subject to Q_{10} temperature dependence depending on the seabed-contact layer temperatures. By this means the parameter count for each sediment process is reduced from a maximum of 6 (one per habitat) to 2.

Additional food web components of the model

Macrophytes

There are many species of littoral macrophytes but large kelp species, with individual plants up to many meters in length, make up a high proportion of the biomass in open water sub-littoral zones. The coarse spatial resolution of the StrathE2E2 means that we cannot aspire to represent the littoral environment, so we base the representation of macrophyte forests on an understanding of the population ecology of kelp species.

Kelps are relatively long-lived plants (up to approximately 10 years depending on species) with a complex physiology and life cycle. Established plants consist of a holdfast for attachment to a rock surface, a stipe, and a frond. Reproduction involves the release of spores which need to settle in a habitat where they can become attached with sufficient light and space to develop. Plants have a particular ability to absorb and store inorganic nitrogen (nitrate and ammonia) independent of carbon assimilation. Typically, nitrogen uptake occurs in the winter and spring and is stored to support biomass growth in the summer when photosynthesis rates are high but environmental concentrations of nutrient are low. As a result, kelp plants show a strong seasonal variation in carbon:nitrogen ratio.

The geographic extent of kelp forests of any given kelp species is generally limited by temperature and light environment (depth and water clarity), distribution of exposed rock or boulder substrate, and exposure to wave action and currents. Wave exposure is particularly significant. There are strong species-specific differences in tolerance to wave action which define both small scale and large scale distributions. Episodic storm damage, seasonal, age- and species-dependent patterns of detachment of whole plants and erosion of frond area are important natural processes for forest dynamics. Settlement of spores and the recruitment of young plants is density-dependent, being limited by space and shading by existing plants.

Biomass densities in kelp forests can be as high as 1 $kgC.m^{-2}$, higher than all of the pelagic food web combined - though obviously the areal extent is much more restricted. Annual primary production rates of kelp forests are hard to measure accurately but may exceed 600 $gC.m^{-2}.y^{-1}$, far exceeding phytoplankton primary production rates on a per unit area basis. In some regions there is a significant industry in mechanical harvesting of kelp as a valuable natural resource for chemical extraction, biofuels and fertilisers. Harvests of up to 100,000 tonnes per year in French and Norwegian waters, for example, exceed the permitted catches of many fish species. However, in other regions such as the UK there is resistance to the establishment of harvesting due to concerns about the loss of biodiversity associated with forest habitats which provide protection for juvenile fish and a wide range of other species. For these reasons, inclusion of kelp forests and harvesting in a model such as StrathE2E2 is a desirable goal.

A model of kelp forest dynamics

A key assumption in StrathE2E2 as a whole is that a single nutrient element (nitrogen) is synonymous with biomass, which is equivalent to assuming a fixed elemental stoichiometry for metabolism. Clearly this is a simplification for all organisms, but tolerable given the coarse groupings of taxa. However, for kelps, the decoupling of nitrogen uptake and biomass accumulation means that the single nutrient simplification is not acceptable. Hence we need a different format for representing kelp forests in the model.

The few models of kelp biomass dynamics that exist in the literature e.g. Aldridge *et al.*, 2012; Broch & Slagstad, 2012) focus on the development (nutrient uptake, carbon assimilation, growth, survival) of individual plants. However, modelling the biomass dynamics of a forest requires either an individual based approach which resolves the interactions between plants (which is costly and impractical in the context of StrathE2E2), or a bulk biomass approach with dimensions that represent the consequences of age composition and the density dependence (resistance to mechanical damage, self-shading). In addition, embedding a kelp forest model in the StrathE2E2 food web requires consideration of the predators on kelp, and on the fate of debris produced by frond erosion and detachment of whole plants.

Within StrathE2E2 we defined the habitat of kelp forests to be delineated by the area of rocky seabed in the shallow/inshore zone. The light environment is then defined by the time-varying turbidity of inshore zone water column layer and the mean seabed depth in the rocky habitat.

Within the inshore zone we added three new state variables: living kelp carbon and nitrogen masses, and kelp debris nitrogen mass. Kelp debris represented the mass of fronds and whole plants detached from the seabed by wave action and senescence.

The nitrogen mass of living and detached kelp forms part of the mass conservation in the whole StrathE2E2 food web, so all gains and losses are accounted for by fluxes from or to other state variables in the model or explicit exports from the system. On the other hand, the carbon mass is not conserved, since carbon is not represented anywhere else in the model. The sole purpose of including kelp carbon mass is to decouple the uptake of dissolved inorganic nitrogen from photosynthesis and regulate its storage in the forest. This was achieved by defining two dynamic parameters Q_N and Q_C which are attenuation coefficients for nitrogen and carbon uptake respectively. Q_N and Q_C are dependent on the forest N:C ratio, such that as the ratio approaches a defined maximum (i.e. internal nitrogen stores in the plants are replete) the uptake rate of dissolved inorganic nitrogen is attenuated to zero and the photosynthetic uptake of dissolved inorganic carbon is defined solely by light and temperature. Conversely, as the N:C ratio approaches a defined minimum (i.e. internal nitrogen stores in the plants are exhausted) nitrogen uptake is defined solely by a type II (Michelis Menten functional response, and carbon uptake is attenuated to zero. The relative uptakes of nitrate and ammonia are governed by preference coefficients as for phytoplankton in the model. The uptake of carbon is governed by a (carbon) density- and light-dependent function, to represent photosynthesis and self-shading by the forest canopy. The permitted bandwidth of the N:C ratio (maximum and minimum) are parameterised directly from published field observations (Johnston *et al.*, 1977; Sjøtun *et al.*, 1996. Wang *et al.*, 2014).

In addition to the inorganic uptake terms, the differential equations for rate of change in both carbon and nitrogen mass of living kelp include terms for predation loss due to grazing, a loss term which represent natural damage and detachment of kelp plants, and a harvesting loss term. In each case, the proportion of mass lost is the same for carbon and nitrogen, i.e. these processes act on whole plant biomass. In the case of carbon, the terms are merely

sinks within the model, but for nitrogen they represent fluxes to other components of the food web – uptake fluxes to the grazer guild, flux to the kelp debris state variable, and an export flux for the harvesting term. The grazing loss term is achieved by including kelp in the predator-prey preference matrix, with the predator defined as being the carnivorous and scavenge feeding benthos guild (e.g. sea urchins, based on literature data on the main species recorded as grazing on kelp). The harvesting loss term is achieved by including 'kelp harvesters' in the set of gears represented in the fishing fleet model, targeting only kelp. The harvesting of kelp is then parameterised in exactly the same way as every other fishery resource guild in the model. The damage and detachment flux to kelp debris is dependent on carbon mass (i.e. forest biomass), and an external driving data time series of significant wave height. The logic here is that the fundamental determinant of destructive loss of biomass is wave action, but this is modulated by the age composition of the forest given that older, larger plants are more susceptible to damage and detachment. Hence, forest biomass here is assumed to be synonymous with the mean age of plants in the forest.

Finally, the differential equation for rate of change in kelp carbon mass includes a loss term to represent the exudation of polysaccharide. This loss term was confined to the carbon mass of the forest since there is no equivalent exudation process involving nitrogen. Literature data indicate that exudation of dissolved organic carbon varies during the life cycle of individual plants such that the proportion of carbon exuded is inversely related to growth rate (Abdullah & Fredriksen, 2004). Hence, we expect old large plants with a low weight-specific growth rate to exhibit high rates of exudation. In the forest model we assume the proportion of carbon biomass exuded per unit time to be a temperature and density dependent process, proportional to forest carbon biomass. As for the wave-dependent destruction rate, biomass is regarded here as being synonymous with the mean age of plants. The carbon loss by this process is a sink term in the model.

Dynamics of kelp debris in the food web

Since we require to account for and conserve nitrogen (but not carbon) mass in the model, we define an additional state variable associated with the kelp forest terms – kelp debris. This is defined only in terms of nitrogen and represents the material generated by the wave-dependent destruction of the kelp forest, and any discarded material from kelp harvesting operations.

Like kelp forests, kelp debris exists only in the shallow inshore zone of the model. We assume no transport of kelp debris to the deep offshore zone. The differential equation for rate of change of kelp debris mass included production terms corresponding to the loss term in the kelp forest equation and any discarding flux from harvesting operations, and loss terms representing temperature-dependent conversion into detritus, grazing loss by scavenging benthos, and an export term from the model representing beach-cast.

Conversion of kelp debris into detritus proceeds as a first-order rate process governed by a temperature-dependent rate coefficient, exactly analogous to all other detrital decay processes in the model. As with the decay of corpses, a proportion of the decay flux is directed to labile detritus (in this case suspended detritus) and the remainder to the refractory detritus pool.

Carnivorous and scavenging benthos are considered to be the only consumers of kelp debris in the food web, defined by an entry in the preference matrix.

Beach-cast – the deposition of kelp debris on the fore-shore – is a well-known phenomenon and instances of mass accumulation of washed-up material are well documented. However, there are few studies of the biomass of beach-cast or of its relation to kelp forest mass or production. One study in New Zealand (Zemke-White *et al.,* 2005) estimated that beach-cast

represented 15% of annual kelp production. In the model, the flux of material from suspended kelp-debris to beach-cast is regarded as a first-order rate process proportional to time-dependent significant wave height, which is supplied as an external driving data set (the same data as are used to drive the wave and density-dependent destruction rate of living kelp forest mass). The flux to beach-cast is an export flux from the modal food web.

Kelp forest balance equations

The rate of change of kelp forest nitrogen (X_N) given a set of k nitrogen nutrient types (N_k) and a set of j grazing predator types (Y_j), is:

$$\frac{dX_N}{dt} = Q_N \sum_k U_{X_N(N_k)} - \sum_j U_{Y_j(X_N)} - \left(W(t)\,\zeta\,X_C{}^2\right)\frac{X_N}{X_C} - H(t)X_N \qquad \text{eqn 17}$$

The rate of change of kelp forest carbon (X_C) given a set of j predator types (Y_j), is:

$$\frac{dX_C}{dt} = Q_C U_{X_C} - \sum_j U_{Y_j(X_N)} \cdot \frac{X_C}{X_N} - \varepsilon(t)X_C{}^2 - \left(W(t)\,\zeta\,X_C{}^2\right) - H(t)X_C \qquad \text{eqn 18}$$

The rate of change of kelp debris (in nitrogen units only) (X_{DN}) given a set of j grazing predator types (Y_j), is:

$$\frac{dX_{DN}}{dt} = \left(W(t)\,\zeta\,X_C{}^2\right)\frac{X_N}{X_C} + \partial\,H(t)X_N - \vartheta(t)\,X_{DN} - \sum_j U_{Y_j(X_N)} - W(t)\,\omega\,X_{DN} \qquad \text{eqn 19}$$

$Uv_1(v_2)$	Flux of nitrogen to a predator (v_1) from prey (v_2). (v_1, v_2 = *kelp and nutrient (X_N, N_k)* or v_1, v_2 = *predator and kelp (Y_j, X_N)*)
Ux_C	Flux of carbon to kelp (X_C)
Q_N	Carbon-dependent attenuation coefficient for nitrogen uptake
Q_C	Nitrogen-dependent attenuation coefficient for carbon uptake
$W(t)$	Time-dependent significant wave height
ζ	Coefficient for density dependent destruction of forest carbon by wave action. Creates a flux to the 'macrphyte debris' class of detritus.
$H(t)$	Harvest ratio (time-dependent rate of biomass harvesting)
$\varepsilon(t)$	Temperature, and hence time-dependent coefficient for density dependent exudation loss of carbon as carbohydrate
$\vartheta(t)$	Temperature, and hence time-dependent coefficient for decay of kelp debris to detritus
∂	Proportion of kelp harvest which is discarded or spilled during the harvesting process.
ω	Scaling coefficient between significant wave height and the proportion of kelp debris washed ashore per day

Uptake flux of kelp by grazing predators ($U_{Y_j(X_N)}$) as in the general equations.

Uptake flux of nutrient (k = nitrate or ammonia) into the kelp nitrogen pool is:

$$U_{XN,(N_k)} = \frac{X_C.N_k.\rho_{X_N(N_k)}.Umax_{X_N}}{N_k + h_{X_N}} \qquad \text{eqn 20}$$

Note that nitrogen uptake is dependent on kelp carbon mass (X_C)

$\rho_{X_N(N_k)}$	Preference of the kelp for the nutrient N_k. The sum of the preference coefficients over all nutrient classes = 1.

$Umax_{X_N}$ Temperature-dependent maximum uptake rate of nutrient by the kelp X_N

h_{X_N} Half-saturation constant for uptake of nutrient by the kelp X_N (temperature independent)

Uptake flux of carbon by the kelp is:

$$U_{X_C} = Min\left\{\left(X_C\ Umax_{X_C}\right), \left(X_C\ Umax_{X_C}\frac{L(t).e^{-X_C.S}}{L_{max}}\right)\right\}$$ eqn 21

$Umax_{X_C}$ Temperature-dependent maximum uptake rate of carbon by the kelp X_C
$L(t)$ Time-dependent light intensity
L_{max} Saturation light intensity for carbon uptake
S Self-shading coefficient

Carbon-dependent attenuation coefficient for nitrogen uptake

$$Q_N = \left\{0 \le \frac{1}{(\Phi_{max}-\Phi_{min})}\left(\Phi_{max} - \frac{X_N}{X_C}\right) \le 1\right\}$$ eqn 22

Nitrogen-dependent attenuation coefficient for carbon uptake

$$Q_C = \left\{0 \le \frac{1}{(\Phi_{max}-\Phi_{min})}\left(\frac{X_N}{X_C} - \Phi_{min}\right) \le 1\right\}$$ eqn 23

Φ_{max} Maximum permitted ratio of kelp nitrogen : carbon molar ratio
Φ_{min} Minimum permitted ratio of kelp nitrogen : carbon molar ratio

Larval stages of benthos guilds

In the prototype model, the two guilds of benthic fauna (suspension/deposit feeders, and carnivore/scavenge feeders) were considered as homogeneous biomass guilds. In contrast, fish were resolved to pelagic larval and juvenile stages, and settled reproductive stages. The main argument for discriminating between these key life stages of fish was that they have distinctly different diet preferences and productivities. However, the same argument applies to the benthos, where the larval stages of most benthic fauna spend a brief period in the plankton (meroplankton) feeding mainly on phytoplankton and detritus in the surface waters before settling back to the seabed. To represent this important life-stage division, larval stages of benthos are implemented as state variables in StrathE2E2.

For each benthos class, between fixed dates of the year, a fixed fraction per day of biomass is transferred to a larval state variable, to represent spawning. Between later fixed dates each year a fixed fraction per day of larval biomass is transferred back to the parent benthos class to represent settlement and recruitment. Larvae consume phytoplankton and suspended detritus in the upper and lower layers of the water column in proportion to the dynamic vertical distributions of these variables, and are subject to passive horizontal mixing between the inshore and offshore zones. The timings of spawning and recruitment are parameterised by reference to annual time series of meroplankton abundances in the Continuous Plankton Recorder (CPR) survey data for the North Sea (Kirby *et al.,* 2008).

Migratory fish

All fish in the prototype model were assumed to be permanently resident in the geographic domain. In fact, some fish species are only seasonal visitors to regions such as might be modelled with StrathE2E2, during the course annual migrations occurring at much larger spatial scales.

The new model code contains a switch to enable or disable a migratory fish state variable. If enabled, then a time series of inward migration flux (inward mass per unit time) needs to be specified as an external driving data-set. Within the model domain, these fish feed, excrete, defecate, die, are eaten by predators, and caught by fisheries in exactly the same way as other fish, with their own set of rate parameters and dietary preferences. However, they do not reproduce by transferring biomass to a larval stage within the model. Between fixed dates, a proportion per day is exported out of the model to represent a seasonal emigration.

Additional ecological fluxes represented in the model

Density dependent mortality rates of phytoplankton

A quadratic mortality term was included in the balance equation for phytoplankton to caricature bloom flocculation and virus epidemics at high algal cell densities (Borlestean *et al.*, 2015; Prairie & Duarte, 1996; Suttle, 1994; Tijdens *et al.*, 2008).

The fate of carcases arising from density dependent mortality

In the prototype model, density dependent mortality was applied to birds & mammals, adult and larvae of pelagic and demersal fish, carnivorous zooplankton, and carnivorous/scavenge feeding benthos. The flux of nutrient generated by these mortality rates was directed to seabed corpses (along with the settling flux of fishery discards). In effect, seabed corpses represent large lumps of detritus.

In extending the model, it made sense to consider whether it was appropriate to include the flux due to density dependent mortality of zooplankton and larvae in the flux to seabed corpses. More likely, the majority of this material will disintegrate or be preyed by scavengers on in the water column rather than on the seabed, though there are accounts of, for example, mass mortalities of jellyfish forming a carpet on the seabed. This is a difficult judgement, but in the new model the mortality flux from carnivorous zooplankton, fish larvae, and larvae of benthos, is diverted to suspended detritus.

Beddington-deAngelis uptake function for top predators

The Holling Type-II equation (Holling, 1959) is widely used to describe the per capita uptake rate (g) of prey (v_2) by a consumer (v_1), in terms of a search rate (c) and a time for processing (b):

$$g_{(v_1)} = \frac{c.v_2}{1+c.b.v_2}$$

eqn 24

This form can be reconfigured as the Michaelis-Menten equation in terms of a prey half-saturation coefficient $h = \frac{1}{c.b}$, and a maximum per capita uptake rate by the predator $Umax = \frac{1}{b}$.

$$g_{(v_1)} = \frac{v_2.Umax_{v_1}}{v_2+h_{v_1}}$$

eqn 25

Incorporating a preference term, the general equation for the flux of ingestate to a predator (v_1) from prey (v_2) is then:

$$U_{v_1(v_2)} = \frac{v_1.v_2.\rho_{v_1(v_2)}.Umax_{v_1}}{v_2+h_{v_1}}$$

eqn 26

where $\rho_{v_1(v_2)}$ is the preference of the predator v_1 for the prey class v_2. For a given predator class, the sum of the preference coefficients over all prey classes = 1. This particular form of preference coefficient is adopted because of the high degree of taxonomic aggregation in the functional guilds of the model (Heath, 2012).

We expect $Umax_{v_1}$ to be temperature-dependent since it depends only on the handling time which should decrease with temperature (so $Umax$ increases). However, we expect the half saturation coefficient to have negligible temperature sensitivity since it depends upon both the search rate and the handling time and these should vary in opposite direction with temperature – search rate should increase with temperature but handling time decrease.

In common with many other aquatic food web models (Gentleman *et al.,* 2003), the Holling Type-II / Michaelis-Menten form was used for all the predator-prey relationships in the prototype version of StrathE2E2. However, the Holling Type-II does not incorporate any regulatory mechanism and hence food chain models based solely on this function exhibit neutral stability or instability. For this reason, the StrathE2E2 model includes quadratic (density-dependent) loss terms for most trophic guilds to represent, for example, competition for an un-modelled resource (e.g. space for sessile taxa), cannibalism (intra-guild predation in the context of our model based on trophic guilds), or incidence of disease epidemics. Other authors have referred to this mathematical process as 'interference' (McCann *et al.*, 1998; Polis & Holt, 1992).

An alternative to mortality regulation is to invoke consumer density-dependence of per capita uptake rate, which suppresses responsiveness by regulating the flux between prey and consumers. This model form is intended to represent sharing of resources, behavioural interference between consumers to their mutual impairment, enhanced escape reactions by prey, sheltering in refuges with increasing predator density (Hill & Weissburg, 2013), or the foraging of predators in a patchy prey environment (Anderson, 2010; Cosner *et al.,* 1999). There are many observational and experimental examples of top-down forced prey behavioural responses to predators of this type, with evidence that they lead to impacts on basal resources – and hence a *de facto* cascade effect (Griffin *et al.*, 2011; Schmitz *et al.*, 2004; Trussell *et al.*, 2006). An established adaptation of the familiar Michaelis-Menten uptake function to confer consumer density-dependent regulation by specifying an additional parameter (γ) is the Beddington-DeAngelis equation (Beddington, 1975; DeAngelis *et al.*, 1975):

$$g_{v_1} = \frac{v_2.Umax_{v_1}}{v_2+\gamma.v_1+h_{v_1}}$$

eqn 27

In StrathE2E2 we adopt this form to represent the consumption of food by the high trophic level predators in the model ecosystem (birds, pinnipeds and cetaceans). This is justified particularly on the grounds that, more than any other guilds in the ecosystem, their foraging behaviour involves cooperative groups of individuals actively seeking out dense patches of prey.

Temperature dependent metabolism of top-predators

For ectothermic plankton, benthos and fish it is clear that background metabolic rates generally scale positively with temperature and a Q_{10} relationship is a reasonable approximation. However, this is not the case for endothermic birds and mammals where metabolic costs scale inversely with temperature (Boyd, 2002; Butler, 2004; Butler & Jones, 1997; Fish, 2000). In the prototype model, neither maximum uptake rate nor background metabolic rates of top predators were subject to temperature dependence. In reality, for endothermic birds and mammals which require to maintain activity at low temperatures, background metabolic rates are <u>inversely</u> related to temperature. This is in contrast to fish and invertebrates where metabolic rates are directly related to temperature. In StrathE2E2, an inverse Q_{10} function is parameterised for birds and mammals to generate ~50% reduction in metabolic rate for a 7.5°C increase in temperature, mimicking the temperature response in cormorants (Enstipp *et al.,* 2006).

Active migrations

Spatially resolved models which include fish and top predators must address the role of active migrations. Some models treat movement as a non-dynamic or 'clockwork' data-driven process, but this is clearly limiting for scenario experiments which aim to explore the properties of the system outside the envelope of observed driving conditions. Movement fundamentally affects regionally-integrated encounter rates between predators and their prey, and hence productivity (Nathan *et al.*, 2008), so needs to be modelled as a dynamic property. However, the motivations for active migrations are many and complex, including time and state-dependent interplays between the feeding, need-to-breed, predator avoidance and environmental tolerances, which are very poorly understood (Berdahl *et al.*, 2016). Individual based methods are an attractive modelling option, but are computationally costly and complicated to integrate with eulerian representations of lower trophic levels (Kay *et al.*, 2017).

As a first order approximation we can assume that active predators are at least motivated by feeding, and are monitoring their environment in an attempt to optimise their distribution in relation to preference-weighted prey concentrations. We achieve this in the model by adopting a ratio-dependent behaviour scheme in which the grazer population attempts to maintain a spatially uniform value of the ratio of their own concentration to the preference-weighted concentration of their prey. The implication of this is that, by means of short-time scale processes such as random searching or diel vertical migrations which are not represented in the model, the grazers are able to monitor concentration gradients in both their prey and their conspecifics, and distribute themselves accordingly (Berdahl *et al.*, 2016). Ratio-dependent behaviour such as this has been widely adopted in ecological models to represent the distribution of grazers (Anderson, 2010; Arditi & Ginzburg, 1989, 2012; Cosner *et al.*, 1999). The methodology for implementing ratio-dependent migrations was different for the vertical and horizontal dimensions.

Vertical migrations

Omnivorous and carnivorous zooplankton, and the planktonic larvae of fish and benthos were assumed to undertake vertical migrations but to be entirely passive in the horizontal. They were represented in the model by depth integrated populations in each horizontal spatial zone. In the offshore zone this meant that we needed to make some assumptions

about vertical distributions between the upper and lower layers of the water column, since the phytoplankton and detritus prey for some of these guilds were explicitly modelled in each depth layer. Grazer vertical distributions also determined the proportional allocation of excretion outputs to depth layers, and only the fraction in the upper layer was eligible for passive mixing exchange with the horizontally connected inshore zone.

We assumed that at daily time scales the populations of these grazers were able to continuously maintain a vertically uniform ratio of their own biomass to their preference-weighted prey concentration. This meant that their vertical distribution was defined to be proportional to that of their prey.

Horizontal migrations

Planktivorous, demersal and migratory fish, and birds and mammals, were assumed to be capable of active horizontal movements, completely independent of hydrodynamics. Given the spatial scale of the horizontal compartments in the model, the time-scales for active horizontal redistributions of biomass were assumed to be longer than the intrinsic daily resolution. Hence, the migrations of these guilds needed to be represented as directed rate processes (horizontal fluxes between spatial compartments) rather than being bound to the distributions of prey as for the vertical migrators.

For each migrating guild, the flux of biomass between spatial compartments was parameterised to be proportional to the horizontal gradient of prey-to-predator biomass ratio, so that predators migrated towards the zone where the prey-predator biomass ratio was highest. As for the vertical migrators, prey density was estimated as the preference-weighted sum over all prey guilds for each predator.

The gradient in prey : predator density ratio (R_Y) is given by:

$$R_Y = ln\left(\frac{\left(\frac{\Sigma_i\left(pref_i \cdot \frac{X_{i,offshore}}{A_{offshore}}\right)}{\left(\frac{Y_{offshore}}{A_{offshore}}\right)}\right)}{\left(\frac{\Sigma_i\left(pref_i \cdot \frac{X_{i,inshore}}{A_{inshore}}\right)}{\left(\frac{Y_{inshore}}{A_{inshore}}\right)}\right)}\right) = ln\left(\frac{\left(\frac{\Sigma_i\left(pref_i \cdot X_{i,offshore}\right)}{\left(Y_{offshore}\right)}\right)}{\left(\frac{\Sigma_i\left(pref_i \cdot X_{i,inshore}\right)}{\left(Y_{inshore}\right)}\right)}\right)$$

eqn 28

provided that:

$\Sigma_i\left(pref_i.X_{i,offshore}\right) > 0$ and $\Sigma_i\left(pref_i.X_{i,inshore}\right) > 0$, and
$Y_{offshore} > 0$ and $Y_{inshore} > 0$

Otherwise,

$R_Y = -R_{Y\,lim}$ if:
$Y_{inshore} = 0$ and $\Sigma_i\left(pref_i.X_{i,inshore}\right) > 0$, or
$\Sigma_i\left(pref_i.X_{i,offshore}\right) = 0$ and $\Sigma_i\left(pref_i.X_{i,inshore}\right) > 0$

$R_Y = +R_{Y\,lim}$ if:
$Y_{offshore} = 0$ and $\Sigma_i\left(pref_i.X_{i,offshore}\right) > 0$, or
$\Sigma_i\left(pref_i.X_{i,inshore}\right) = 0$ and $\Sigma_i\left(pref_i.X_{i,offshore}\right) > 0$

Otherwise,

$$R_Y = 0$$

Here, $X_{i,offshore}$ and $X_{i,inshore}$ are the masses (mMN) of the prey guild i in the offshore and inshore zones respectively, $Y_{offshore}$ and $Y_{inshore}$ are the corresponding masses of the predator, $pref_i$ is the preference of the predator Y for each prey type i, and $A_{offshore}$ and $A_{inshore}$ are the surface areas of the offshore and inshore zones.

$R_{Y\,lim}$ is a fixed value of R_Y to achieve the extreme eventualities of recolonization of a zone devoid of Y provided that food is present, or evacuation of Y from a zone where food becomes absent. In reality these conditions can never be met provided that positive non-zero values are provided for the initial masses of the predators in the model.

Then, the directed migration fluxes (mMN.d^{-1}) from the offshore to the inshore zone ($M_{Y,offshore\text{-}inshore}$), and conversely from the inshore to the offshore zone ($M_{Y,inshore\text{-}offshore}$) are given by:

$$M_{Y,offshore-inshore} = \begin{vmatrix} Y_{offshore} \cdot \dfrac{k_Y}{A_{offshore}} \cdot R_Y{}^2 \, , \ R_Y < 0 \\ \\ 0 \ otherwise \end{vmatrix}$$

eqn 29

$$M_{Y,inshore-offshore} = \begin{vmatrix} Y_{inshore} \cdot \dfrac{k_Y}{A_{inshore}} \cdot R_Y{}^2 \, , \quad R_Y > 0 \\ \\ 0 \ otherwise \end{vmatrix}$$

eqn 30

where k_Y is a predator-specific scaling coefficient.

Parameterising the proportion of resource guild biomass which is accessible to fishing gears

The prototype version of the ecology model assumed that all of the biomass of each fishery resource guild was accessible to fishing gears. For the pelagic and demersal fish guilds this was clearly a simplification, but defensible since the biomass of species which appear in scientific surveys but not in commercial catches is only a small fraction of the total. However, this was plainly not the case for the benthos, carnivorous zooplankton or bird and mammal guilds. Here, the species targeted or accidentally caught by fisheries constitute only a small fraction of the functional guild biomass. For example, harvested bivalves represent only a very small proportion of all filter and deposit feeding benthos. This meant that a) harvest rates required to generate realistic catches from the whole guild were orders of magnitude lower than those deduced from assessments of the target species themselves and, b) in principle the entire functional guild could be harvested to extinction in the model whilst this could never happen in practice.

In StrathE2E2, rather than explicitly modelling the biomass of harvested and non-harvested guilds as separate state variables thereby incurring many additional parameters, we specify two additional terms for each resource guild to parameterise the proportion of biomass accessible to the fisheries. First, we define a threshold of biomass density (m^{-2}) below which none is accessible to the fishery. This would represent a situation where all the species within a guild which are targeted by fishing had been exhausted, or where a proportion of the harvestable stock lives in an area which is inaccessible to fishing gears. Second, we define a

maximum proportion of the guild biomass which is potentially accessible to fishing in an unfished system. The accessible proportion is represented as increasing asymptotically towards this maximum as biomass increases beyond the threshold. For the benthos and carnivorous zooplankton guilds in the new model, we expect the threshold values to represent a high proportion of typical guild biomass, and the maximum accessible fraction to be relatively small. For the fish guilds, we expect a low threshold and a high maximum proportion.

For fish guilds in the North Sea demonstration model for example, values of the biomass threshold parameters were estimated from the catch per unit swept area in research vessel trawl surveys, of species which were not represented in the commercial catch records. For the benthos guilds, the biomass threshold was estimated from the ICES North Sea Benthos Survey data, excluding the commercially exploited species. For the carnivorous zooplankton guild the biomass threshold was taken to be the minimum annual average biomass density estimated by the Continuous Plankton Recorder Surveys, which does not record any catches of squid. For each guild, the maximum accessible fraction (p_{max}) was treated as a fitting parameter in the model. The form of the relationship in each case was:

$$p(w) = max\left\{0, \left(p_{max} \cdot \left(1 - \frac{a_w.B_{lim}}{B(w)}\right)\right)\right\}$$

<div align="right">eqn 31</div>

or

$$B(w)_{harvestable} = p(w) \cdot B(W) = max\left\{0, \left(p_{max} \cdot \left(B(w) - (a_w \cdot B_{lim})\right)\right)\right\}$$

<div align="right">eqn 32</div>

where $p(w)$ is the fraction of guild biomass accessible to the fishery in zone w of area a_w, $B(w)$ is the guild biomass in the zone, B_{lim} is the threshold biomass density (m^{-2}) below which there is no harvestable fraction remaining, and $B(w)_{harvestable}$ is the biomass available to the fishery.

References

Abdullah, M.I. & Fredriksen, S. (2004). Production, respiration and exudation of dissolved organic matter by the kelp *Laminaria hyperborea* along the west coast of Norway. *Journal of the Marine Biological Association of the UK*, 84, 887-894.

Aldridge, J., van de Molen, J. & Forster, R. (2012). Wider ecological implications of macroalgae cultivation. The Crown Estate, 95 pp.

Anderson, J.J. (2010). Ratio- and predator-dependent functional forms for predators optimally foraging in patches. *American Naturalist*, **175**, 240-249.

Arditi, R. & Ginzburg, L.R. (1989). Coupling in predator-prey dynamics: ratio dependence. *Journal of Theoretical Biology*, **139**, 311-326.

Arditi, R. & Ginzburg, L.R. (2012). *How species interact: altering the standard view on trophic ecology*. Oxford University Press, NY, 204pp.

Arndt, S., Jørgensen, B.B., LaRowe, D.E., Middelburg, J.J., Pancost, R.D. & Regnier, P. (2013). Quantifying the degradation of organic matter in marine sediments: A review and synthesis. *Earth Science Reviews,* **123**, 53-86.

Beddington, J.R. (1975). Mutual interference between parasites or predators and its effect on searching efficiency. *Journal of Animal Ecology*, **51**, 331-340.

Berdahl, A., van Leeuwen, A., Levin, A.A. & Torney, C.J. (2016). Collective behaviour as a driver of critical transitions in migratory populations. *Movement Ecology*, **4**, 18, 1-12.

Billen, C. (1982). Modelling the processes of organic matter degradation and nutrient recycling in sedimentary systems. In D.B. Nedwell and C.M. Browm (eds) *Sediment Microbiology*, Academic Press, London, pp 15-52.

Borlestean, A., Frost, P.C. & Murray, D.L. (2015). A mechanistic analysis of density dependence in algal population dynamics. *Frontiers in Ecology and Evolution, 3*:37, 1-9. doi: 10.3389/fevo.2015.00037

Boyd, I.L. (2002). Estimating food consumption of marine predators: Antarctic fur seals and macaroni penguins. *Journal of Applied. Ecology, 39*, 103-119.

Broch, O.J. & Slagstad, D. (2012). Modelling seasonal growth and composition of the kelp *Saccharina latissimi*. Journal of. Applied Phycology 24, 759-776.

Butler, P.J. (2004). Metabolic regulation in diving birds and mammals. *Respiration, Physiology and Neurobiology, 141*, 297-315.

Butler, P.J. & Jones, D.R. (1997). The physiology of diving of birds and mammals. *Physiology Reviews, 77*, 837-899.

Canfield, D.E. (1994). Factors influencing organic carbon preservation in marine sediments. *Chemical Geology*, **114**, 315-329.

Cosner, C., DeAngelis, D.L., Ault, J.S. & Olson, D.B. (1999). Effects of spatial groupings on the functional response of predators. *Theoretical Population Biology*, **56**, 65-75.

DeAngelis, D.L., Goldstein, R.A. & O'Neill, R.V. (1975). A model for trophic interaction. *Ecology*, **56**, 881–892.

Enstipp, M.R., Grémillet, D. & Jones, D.R. (2006). The effects of depth, temperature and food ingestion on the foraging energetics of a diving endotherm, the double-crested cormorant (*Phalacrocorax auritus*). *Journal of Experimental Biology, 209*, 845-859.

Fish, E.F. (2000). Biomechanics and energetics in aquatic and semiaquatic mammals: platypus to whale. *Physiological and. Biochemical Zoology, 73*, 683-698.

Gentleman, W., Leising, A., Frost, B., Strom, S. & Murray, J. (2003). Functional responses for zooplankton feeding on multiple resources: a review of assumptions and biological dynamics. *Deep Sea Res. II*, **50**, 2847–2875.

Griffin, J.N., Butler, J., Soomdat, N.N., Brun, K.E., Chejanovski, Z.A. & Silliman, B.R. (2011) Top predators suppress rather than facilitate plants in a trait-mediated tri-trophic cascade. *Biology Letters, 7*, 5710-5713.

Heath, M.R. (2012). Ecosystem limits to food web fluxes and fisheries yields in the North Sea simulated with an end-to-end food web model. *Progress in Oceanography* (Special issue: End-to-end modelling: Towards Comparative Analysis of Marine Ecosystem Organisation), **102**, 42-66.

Hill, J.M. & Weissburg, M.J. (2013). Predator biomass determines the magnitude of non-consumptive effects (NCEs) in both laboratory and field environments. *Oecologia*, **172**, 79-91.

Holling, C.S. (1959). Some characteristics of simple types of predation and parasitism. *Canadian. Entomologist*, **91,** 385-389.

Johnston, C.S., Jones, R.G. & Hunt, R.D. (1977). A seasonal carbon budget for a laminarian population in a Scottish sea-loch. *Helgoländer wissenschaftliche Meeresuntersuchungen* 30, 527-545.

Kay, S.L., Fischer, J.W., Monaghan, A.J., Beasley, J.C., Boughton, R., Campbell, T.A., Cooper, S.M., Ditchkoff, S.S., Hartley, S.B., Kilgo, J.C., Wisely, S.M., Wyckoff, A.C., VerCauteren, K.C. & Pepin, K.M. (2017). Quantifying drivers of wild pig movement across multiple spatial and temporal scales. *Movement Ecology,* **5**:14, 15pp.

Kirby, R.R., Beaugrand, G. & Lindley, J.A. (2008). Climate-induced effects on the meroplankton and the benthic-pelagic ecology of the North Sea. *Limnology and Oceanography*, **53**, 1805-1815.

McCann, K.S., Hastings, A. & Strong, D.R. (1998). Trophic cascades and trophic trickles in pelagic food webs. *Proceedings of the Royal Society of London B,* **265**, 205-209.

Nathan, R., Getz, W.M., Revilla, E., Holyoak, M., Kadmon, R., Saltz, D. & Smouse, P.E. (2008). A movement ecology paradigm for unifying organismal movement research. *Proceedings of the National Academy of Sciences*, **105**, 19052-19059.

Olsgard, F., Schaanning, M.T., Widdicombe, S., Kendall, M.A., Austen, M.C. (2008). Effects of bottom trawling on ecosystem function. *Journal of Experimental Marine Biology and Ecology*, **366**, 123-133.

Polis, G.A. & Hort, R.D. (1992). Intra-guild predation: The dynamics of complex trophic interactions. *Trends in Ecology and Evolution*, **7**, 151–154.

Prairie, Y.T. & Duarte, C.M. (1996). Weak density-dependence and short-term perturbations as determinants of phytoplankton temporal dynamics. Ecoscience, **3**, 451-460.

Schmitz, O.J., Krivan, V. & Ovadia1, O. (2004). Trophic cascades: the primacy of trait-mediated indirect interactions. *Ecology Lett*ers, **7**, 153–163.

Trussell, G.C., Ewanchuk, P.J. & Matassa, C.M. (2006). Habitat effects on the relative importance of trait and density-mediated indirect interactions. *Ecology Lett*ers, **9**, 1245–1252.

Serpetti, N., Heath, M., Rose, M. and Witte, U. (2012). Mapping organic matter in seabed sediments off the north-east coast of Scotland (UK) from acoustic reflectance data. *Hydrobiologia,* **680**, 265–284.

Serpetti, N., Witte, U., Heath, M. (2016). Statistical modelling of variability in sediment-water nutrient and oxygen fluxes. *Frontiers in Earth Science*, 4:65, 1-17. doi: 10.3389/feart.2016.00065

Sjøtun, K., Fredriksen, S. & Rueness, J. (1996). Seasonal growth and carbon and nitrogen content in canopy and first-year plants of *Laminaria hyperborea* (Laminariales, Phaeophyceae). *Phycologia* 35, 1-8.

Suttle, C.A. (1994). The significance of viruses to mortality in aquatic microbial communities. *Microbial Ecology*, **28**, 237-243.

Tijdens, M., Van de Waal, D.B., Slovackova, H., Hoogveld, H.L. & Gons, H.J. (2008). Estimates of bacterial and phytoplankton mortality caused by viral lysis and microzooplankton grazing in a shallow eutrophic lake. *Freshwater Biology*, 53, 1126–1141

Wang, X., Broch, O.J., Forbord, S., Handa, A., Skjermo, J., Reitan, K.I., Vadstein, O. & Olsen, Y. (2014). Assimilation or inorganic nutrients from salmon (*Salmo salar*) farming by the macroalgae (*Saccharina latissimi*) in an exposed coastal environment: implications for integrated multi-trophic aquaculture. *Journal of Applied Phycology* 26, 1869-1878.

Zemke-White, W.L., Speed, S.R. & McClary, D.J. (2005). Beach-cast seaweed: a review. *New Zealand Fisheries Assessment Report* 2005/44. 47pp.